



Review

The composition-explicit distillation curve technique: Relating chemical analysis and physical properties of complex fluids[☆]

Thomas J. Bruno^{*}, Lisa S. Ott, Tara M. Lovestead, Marcia L. Huber

Thermophysical Properties Division, National Institute of Standards and Technology, Boulder, CO, USA

ARTICLE INFO

Article history:

Available online 17 November 2009

Keywords:

Chemical analysis
Distillation curve
Enthalpy of combustion
Petroleumomics
Trace analysis

ABSTRACT

The analysis of complex fluids such as crude oils, fuels, vegetable oils and mixed waste streams poses significant challenges arising primarily from the multiplicity of components, the different properties of the components (polarity, polarizability, etc.) and matrix properties. We have recently introduced an analytical strategy that simplifies many of these analyses, and provides the added potential of linking compositional information with physical property information. This aspect can be used to facilitate equation of state development for the complex fluids. In addition to chemical characterization, the approach provides the ability to calculate thermodynamic properties for such complex heterogeneous streams. The technique is based on the advanced distillation curve (ADC) metrology, which separates a complex fluid by distillation into fractions that are sampled, and for which thermodynamically consistent temperatures are measured at atmospheric pressure. The collected sample fractions can be analyzed by any method that is appropriate. The analytical methods we have applied include gas chromatography (with flame ionization, mass spectrometric and sulfur chemiluminescence detection), thin layer chromatography, FTIR, corrosivity analysis, neutron activation analysis and cold neutron prompt gamma activation analysis. By far, the most widely used analytical technique we have used with the ADC is gas chromatography. This has enabled us to study finished fuels (gasoline, diesel fuels, aviation fuels, rocket propellants), crude oils (including a crude oil made from swine manure) and waste oils streams (used automotive and transformer oils). In this special issue of the Journal of Chromatography, specifically dedicated to extraction technologies, we describe the essential features of the advanced distillation curve metrology as an analytical strategy for complex fluids.

Published by Elsevier B.V.

Contents

1. Introduction	2704
1.1. Advanced distillation curve method	2704
2. Applications of the ADC method	2706
2.1. Volatility and detailed chemical analysis	2706
2.2. Hydrocarbon type analysis—aviation fuels	2707
2.3. Volatility and energy content	2708
2.4. Tracking selected components	2709
2.5. Detection of azeotropes	2710
2.6. Study of azeotropes	2711
2.7. Volatility and chemical stability	2711
2.8. Volatility and corrosivity	2712
3. Thermodynamic modeling	2712
4. Conclusion	2715
References	2715

[☆] Contribution of the United States government; not subject to copyright in the United States.

^{*} Corresponding author. Tel.: +1 303 497 5158; fax: +1 303 497 5927.

E-mail address: bruno@boulder.nist.gov (T.J. Bruno).

1. Introduction

This special issue of the Journal of Chromatography provides the opportunity to highlight the importance of separation/extraction processes in general, and how the specific techniques of chemical separations can be used to solve laboratory and industrial problems. The importance of separation processes cannot be understated, since nearly 40% of the cost of any chemical product is directly attributable to the separation processes used in their production [1]. These processes include distillation, extraction, adsorption, diffusion and zone refining, to mention just a few. For industrial applications, distillation has long been the dominant separation process, in terms of the overall number of units implemented, and in terms of total capital investment. The relative simplicity and efficiency, and the long term experience base makes distillation the first choice in the chemical processing industry, even when other methods might be viable.

Aside from the chemical production aspects, the dependence of separations techniques on intermolecular interactions has also provided the metrology to study chemical properties, and to determine how such properties relate to the constituents of mixtures. The application of chromatographic methods for physicochemical measurements, for example, has been well known for nearly 50 years [2]. Thermodynamic parameters measured by chromatography have been validated by other techniques such as spectroscopy and calorimetry. In a similar manner, we can use distillation as a measurement method, one that is especially applicable for complex fluids. Here, the relationship between composition on the one hand and vapor liquid equilibrium on the other (both controlling factors in distillation) furnishes us with a bridge between analytical chemistry and thermophysical property measurement [3,4].

Since complex, multi-component fluid mixtures vaporize over a range of temperatures, the only practical avenue to assess the vapor liquid equilibrium (VLE) is the measurement of the distillation or boiling curve [5]. The classical distillation curve of a fluid is a graphical depiction of the boiling temperature of the mixture plotted against the volume fraction distilled. This volume fraction is usually expressed as a cumulative percent of the total volume. One most often thinks of distillation curves in the context of petrochemicals and petroleum refining, but such curves are of great value in assessing the properties of any complex mixture [6–9]. Indeed, the measurement of distillation curves has been part of complex fluid specifications for a century (typically listed in specifications and data sheets as the fluid volatility), and they are inherent in the design and application of all fuels. Despite this importance, the standard methods for the measurement of such curves have been plagued with systematic uncertainty and bias, and an absence of any link to fluid theory [10]. This has led many petroleum scientists and engineers to consider the measurement of distillation curves to be virtually meaningless, valuable only because everybody has done it the same way. Moreover, the standard metrology has always ignored the compositional aspects that are so important; distillation is really all about composition.

We recently introduced an improved method, called the composition-explicit or advanced distillation curve (ADC) metrology, as a means to characterize complex fluids [11–14]. The ADC approach addresses many of the shortcomings of the classical distillation methods described above. Most important, we incorporate a composition-explicit data channel for each distillate fraction (for both qualitative, quantitative and trace analysis). Sampling very small distillate volumes (5–25 μL) yields a composition-explicit data channel with nearly instantaneous composition measurements. Chemical analysis of the distillate fractions allows for determination of how the composition of the fluid varies with vol-

ume fraction and distillation temperature, even for complex fluids. These data can be used to approximate vapor liquid equilibrium of complex mixtures, and present a more complete picture of the fluid under study. The ADC approach provides consistency with a century of historical data, an assessment of the energy content of each distillate fraction, and where needed, a corrosivity assessment of each distillate fraction. Suitable analytical techniques include gas chromatography with either flame ionization detection (GC-FID) or mass spectral detection (GC-MS), element specific detection (such as gas chromatography with sulfur or nitrogen chemiluminescence detection, GC-SCD or GC-NCD), Karl Fisher coulombic titrimetry, refractometry, and Fourier transform infrared spectrometry (FTIR) [15,16].

Another advantage of the ADC approach is that it provides temperature, volume and pressure measurements of low uncertainty, and the temperatures that are obtained are true thermodynamic state points that can be modeled with an equation of state. In fact, we have used the ADC method to develop chemically authentic surrogate mixture models for the thermophysical properties of a coal-derived liquid fuel, a synthetic aviation fuel, S-8, and rocket propellants RP-1 and RP-2 [11–14,17–19]. The ability to couple the compositional data with the thermal data gives us access to numerous material dependent quantities, and the ability to relate them to the mixture volatility. We will illustrate this in the selected examples that follow.

1.1. Advanced distillation curve method

The apparatus and procedure for the measurement of the composition ADC have been discussed in detail elsewhere; only a brief description will be provided here [11,13]. The apparatus is depicted schematically in Fig. 1. The stirred distillation flask is placed in an aluminum heating jacket contoured to fit the flask. The aluminum jacket serves to integrate out temperature gradients in all but the vertical direction, in which direction a gradient must exist to provide mass transfer. The jacket is resistively heated, controlled by a model predictive PID controller that applies a precise thermal profile to the fluid [14]. Three observation ports are provided in the insulation to allow penetration with a flexible, illuminated borescope. The ports are placed to observe the fluid in the boiling flask, the vapor space at the top of the boiling flask, and the vapor in the distillation head (at the bottom of the take-off).

Above the distillation flask, a centering adapter provides access for two thermally tempered, calibrated thermocouples that enter the distillation head. Calibration is normally done with a triple point cell that can be traced to a NIST standard. One thermocouple (T1) is submerged in the fluid and the other (T2) is centered in the head at the low point of distillate take-off. Also in the head is a stainless steel capillary tube that provides an inert gas blanket for use with thermally unstable fluids. Distillate is taken off the flask with the distillation head, into a forced-air condenser that is chilled with a vortex tube [20–22]. The vortex tube is a device that produces a stream of hot and cold air from an ordinary shop air source. We use air as the cooling medium because it is easily controlled, and it avoids the problems associated with a water flow. Water cooled condensers can cause glassware cracking due to the high heat capacity of water, and always involve the potential for leaks.

Following the condenser, the distillate enters a new transfer adapter that allows instantaneous sampling of distillate for analysis. The flow path of the distillate is focused to drop into a 0.05 mL “hammock” that is positioned directly below the flow path. A crimp cap or screw cap fixture is incorporated as a side arm of the adapter. This allows a replaceable silicone or Teflon septum (of the type used for chromatographic automatic sampler vials) to be positioned in

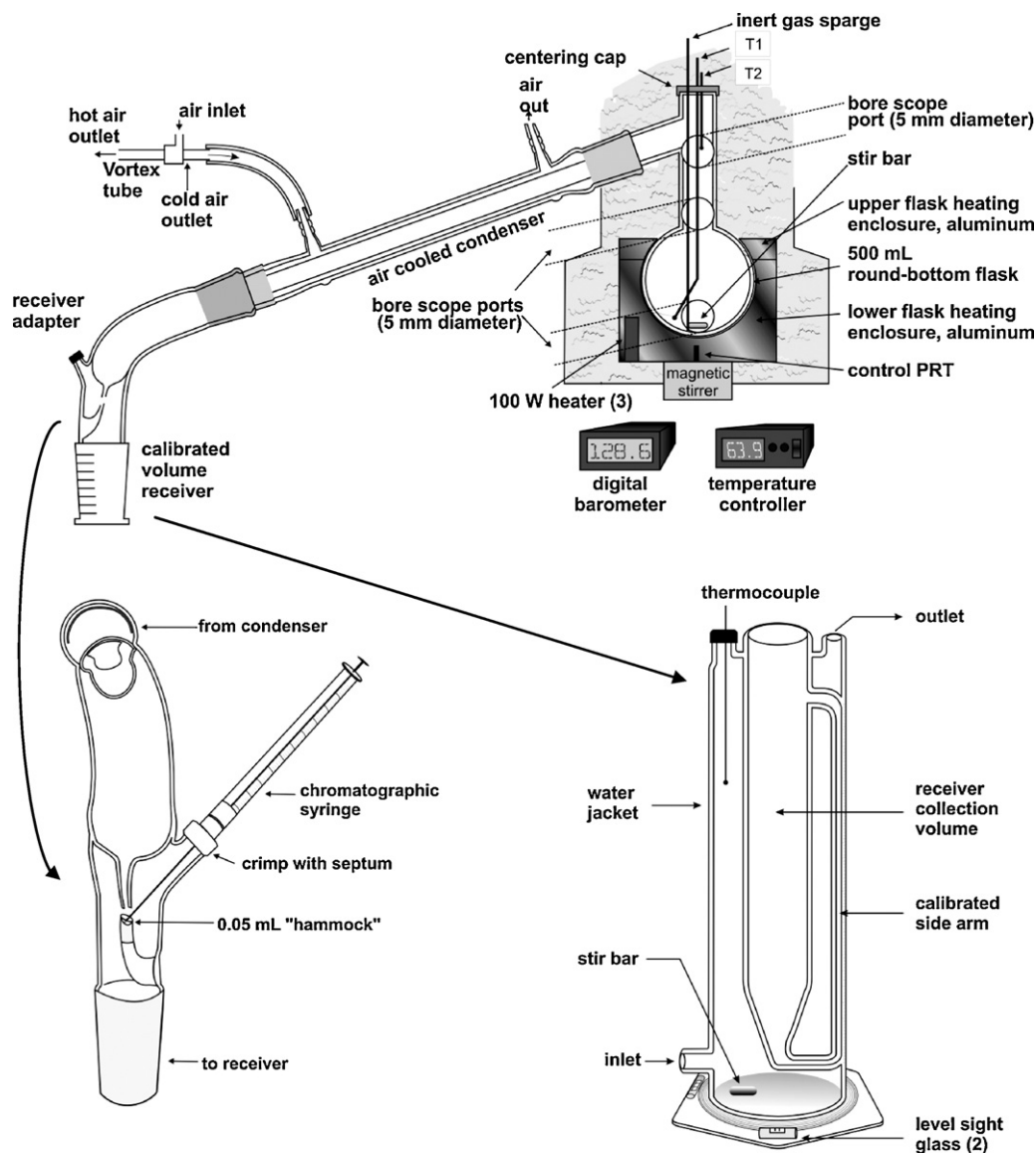


Fig. 1. Schematic diagram of the overall apparatus used for the measurement of distillation curves. Expanded views of the sampling adapter and the stabilized receiver are shown in the lower half of the figure.

line with the hammock. The distance from the crimp cap to the base of the hammock is suited to the needle length of typical gas chromatographic syringes. To sample the distillate, one simply positions the chromatographic syringe, preferably equipped with a blunt tipped needle, in the well of the hammock.

When the sample leaves the adapter, it flows into the calibrated, level-stabilized receiver for a precise volume measurement. Constructed of glass, this receiver consists of a central volume that gradually decreases in diameter at the base, and connects to a small-diameter side arm sight glass that is calibrated. The side arm stabilizes the fluid level for a precise volume measurement as the distillation proceeds. The large inner volume and the sight glass are enclosed in a water jacket that contains a thermometer and a magnetic stir bar for circulation. When surface tension effects become problematic (as with mixtures of polar and nonpolar constituents), we use a receiver with volumes of equal diameters.

Since the measurements of the distillation curves are performed at ambient atmospheric pressure (measured with an electronic barometer), temperature readings are usually corrected for what should be obtained at standard atmospheric pressure (1 atm = 101.325 kPa) [23]. This adjustment is done with the NIST-

modified Sydney Young equation [23–27]. The typical temperature uncertainty is less than $0.3\text{ }^{\circ}\text{C}$ (with 2σ), the volume uncertainty is 0.05 mL, and the uncertainty in the pressure measurement is 0.003 kPa.

To measure a distillation curve, fluid (40–200 mL) is placed in the distillation flask and the heating profile begins. We alluded to this earlier when mention was made of the model predictive temperature controller [14]. The thermal profile typically has the sigmoidal shape of a distillation curve, but continuously leads the fluid by $\approx 20\text{ }^{\circ}\text{C}$. Thus, the typical vaporization behavior of the fluid is approximated in a model, and applied to the surroundings of the flask. This is done to ensure a constant mass flow rate through the apparatus.

For each ADC measurement, we can record a data grid consisting of: T_k , the temperature of the fluid (measured with T1), T_h , the temperature in the head (measured with T2), the corresponding fluid volume, the elapsed time, and the external (atmospheric) pressure. Along with these data, one withdraws a sample for detailed analysis. This procedure provides access to the detailed composition, energy content, corrosivity, etc., corresponding to each datum in the grid.

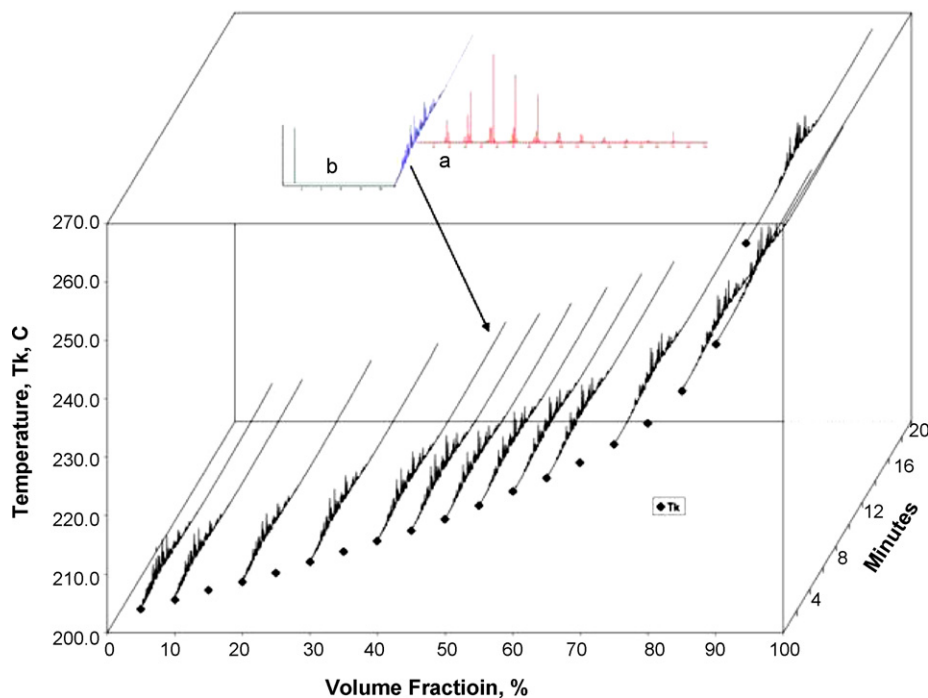


Fig. 2. A distillation curve for RP-1 showing T_k against volume fraction in the x - y plane, and the composition as measured by gas chromatography along the “ z ” axis, represented as retention time against peak intensity. Inset “a” above shows the mass spectrum of the major peak of the 40% fraction, n -dodecane; inset “b” shows a total sulfur chromatographic peak.

2. Applications of the ADC method

2.1. Volatility and detailed chemical analysis

A detailed chemical analysis coupled with physical property information is very helpful if not essential in QA/QC for complex fluids. Examples can be drawn from the kerosenes that are used for jet fuels and rocket propellants.

While modern rocket motors can operate on either a liquid or a solid fuel package, the former is more easily controlled and flexible. This led to the development of RP-1 kerosene in the 1950s, which continues to be widely used [28]. The desire in recent years to use rocket motors many times has led to reformulations of RP-1 with low sulfur, olefin and aromatic content. Reformulation has required a reassessment of the physical properties, for which we have used the ADC metrology. We show in Fig. 2 a distillation curve of RP-1 that has the composition measurement superimposed [12]. First, focusing on the plot of T_k against volume fraction, we note that the plot shape is a subtle sigmoid, characteristic of a complex fluid with many components. ADC data such as these are used in the design and specification of many engine operational parameters, and in equation of state-based model development. Since the T_k data are thermodynamic state points, the plot represents a cut through the fluid phase diagram that has theoretical meaning.

The composition-explicit channel provides additional information for the data grid. In Fig. 2, the composition is shown for selected temperature–volume pairs as measured by GC-MS. Additional detail is shown in the inset, where the mass spectrum of the largest peak is identified as n -dodecane. Clearly, the application of GC-MS can be used to any degree of detail that is desired. We can also use element specific detection in many cases to answer specific questions. As discussed above, RP-1 has been reformulated to have lower sulfur content, in order to decrease corrosivity and metal erosion in the engines. Thus, the application of sulfur analysis with a sulfur chemiluminescence detector is of critical importance. This analysis is also shown in the inset, allowing a breakdown of the

sulfur budget on the basis of fraction volatility. This compositional information is now joined with a temperature grid measurement discussed above; the temperature, pressure and composition can all be modeled with an equation of state, as discussed later.

We can provide a more detailed picture of the results from the composition-explicit channel in the examination of the distillate fractions of a sample of Jet-A (flash point $\approx 38^\circ\text{C}$, freezing temperature -40°C), the major gas turbine aviation kerosene used commercially in the United States, with a consumption of 800 billion liters in 2006. To ensure an adequate supply for commercial markets, the overall specifications of Jet-A are relatively wide in terms of thermophysical properties. This is reflected in sometimes widely varying distillation curves that can be measured for acceptable, in-specification fluids. It can therefore be difficult to define a “typical” sample of Jet-A, however in earlier work we measured the distillation curves of a composite sample of Jet-A. This sample was prepared by combining aliquots from approximately ten separate lots of Jet-A. We show in Fig. 3 a series of chromatograms measured with a FID of the distillate fractions for this composite sample of Jet-A [29,30]. The time axis is from 0 to 12 min for each chromatogram, and the abundance axis is presented in arbitrary units of area counts (voltage slices). It is clear that although there are many peaks on each chromatogram (30–40 major peaks and 60–80 minor and trace peaks), these chromatograms are much simpler than those of the neat fluids, which can contain 500–800 major peaks. At the very start of each chromatogram is the solvent front, which does not interfere with the sample. One can follow the progression of the chromatograms in Fig. 3 as the distillate fraction becomes richer in the heavier components. This figure illustrates just one chemical analysis strategy that can be applied to the distillate fractions. It is possible to use any analytical technique that is applicable to solvent borne liquid samples that might be desirable for a given application. With this approach, we can track the appearance of the lightest components early in the distillation, and how these components disappear as the heavier components grow in.

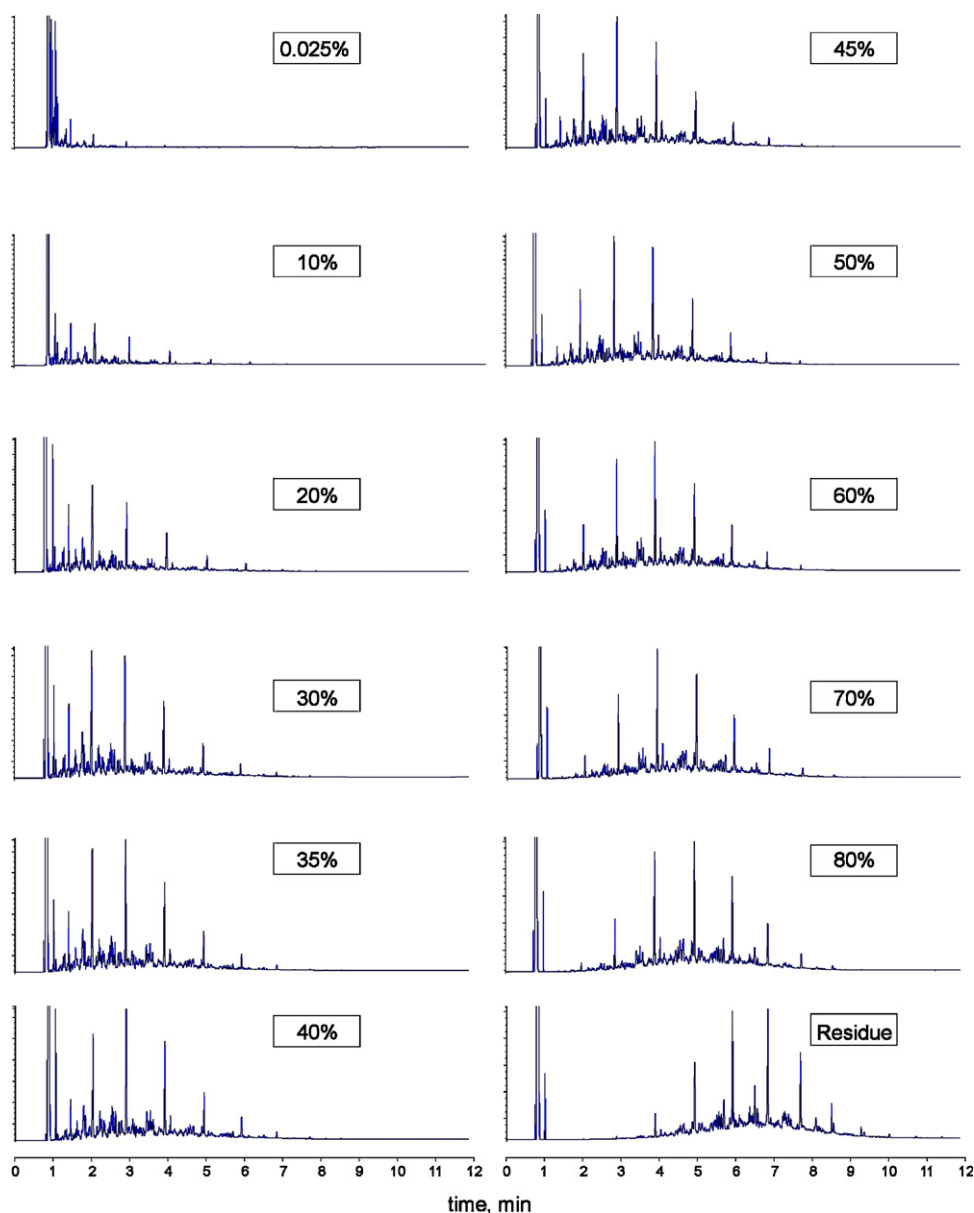


Fig. 3. Chromatograms of distillate fractions of a typical Jet-A sample presented in arbitrary units of intensity (from a flame ionization detector) plotted against time. The details of the chromatography are discussed in the text.

2.2. Hydrocarbon type analysis—aviation fuels

It is not always necessary to include a detailed analysis for each line of the data grid. It is often of value to simply classify the chemical families that are present. This is possible with a variety of methods. We routinely apply a mass spectrometric moiety classification method (similar to ASTM Method D-2789), in which one characterizes hydrocarbons into six types: paraffins, monocycloparaffins, dicycloparaffins, alkylbenzenes, indanes and tetralins (grouped), and naphthalenes. While not without its limitations, and certainly not the only such test used for gross characterization, it can be used reliably as a comparative tool for evaluations between individual batches of complex fluids. We illustrate the application of this approach to the comparison of the distillation curve data grid of two aviation turbine fuels, JP-8 and S-8 [31].

JP-8 is the major turbine fuel currently used by the United States military (MIL-DTL-83133), a kerosene fraction that has a higher flash point than the main military predecessor, JP-4. JP-8 was first introduced at NATO bases in 1978 and is currently the US Air Force's

primary fuel, and the primary fuel for US Navy shore-based aviation. JP-8 is very similar to Jet-A-1, the most common commercial gas turbine fuel in Europe, with the major differences being in the additive package. Note that Jet-A and Jet-A-1 differ in an additive that decreases the freezing point of Jet-A-1 to -47°C . JP-8 also typically contains an icing inhibitor, corrosion inhibitor/lubricity enhancer and anti-static additive. Significant variability is observed in the composition of JP-8 (and the Jet-A fluid discussed above). Much of this variability is intentional, to allow for an ample supply. Additional variability found in JP-8 results from the additive package, which is often splash blended at the flight line. Understanding the composition and variability has always been important, and is currently becoming even more critical, as detailed in the next paragraph.

There is a desire in the United States defense community to utilize JP-8 as the main battlefield fuel for all vehicles, not only for aviation applications but also for ground based forces. Environmental concerns and the potential of disruptions in supply have led to the development of synthetic aviation fuels. Synthetics are

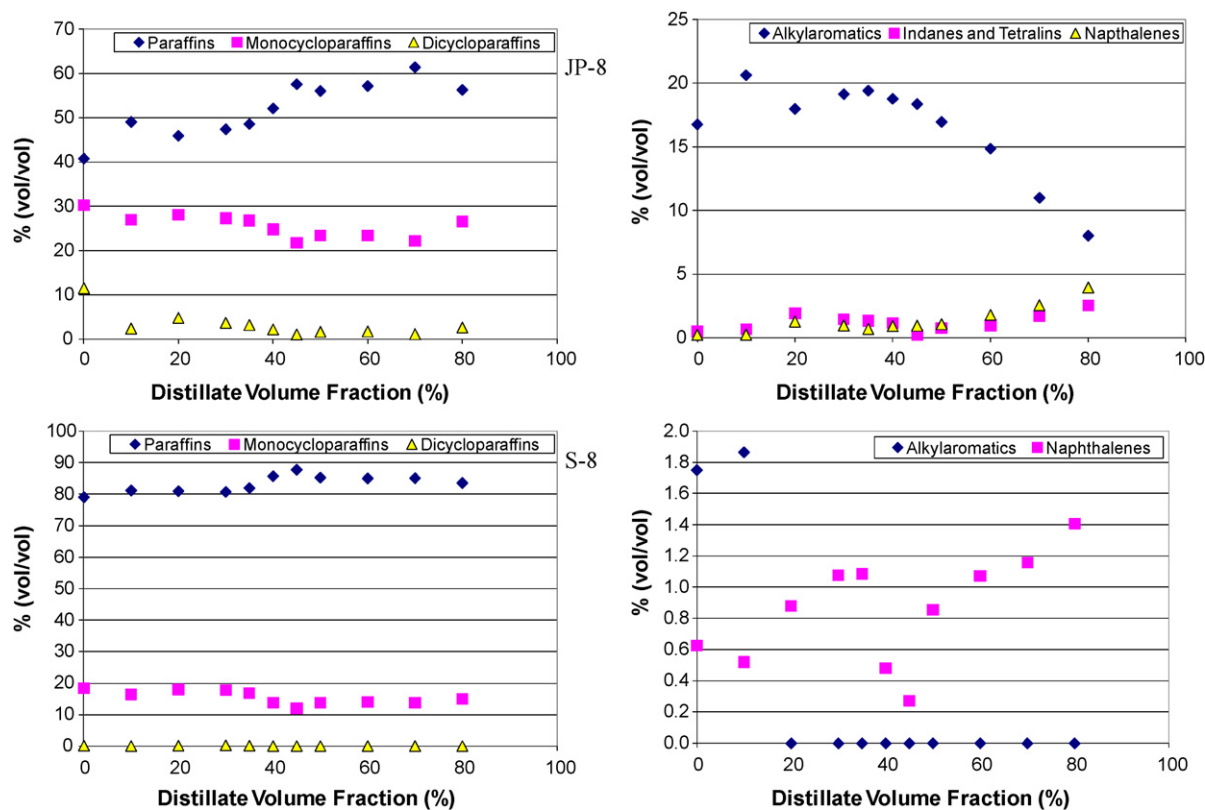


Fig. 4. Plots showing the distribution of chemical families present in aviation fuels JP-8 and S-8, as determined by mass spectrometry.

of interest as extenders and even as drop-in replacements for JP-8. One such fuel made from natural gas (with the Fischer Tropsch process) is designated as S-8 (the “S” referring to synthetic; CAS No. 437986-20-4) [12]. This fluid is a hydrocarbon mixture rich in C7 to C18 linear and branched alkanes, with few if any aromatics. It has a flash point range of between 37.8 and 51.8 °C, an autoignition temperature of 210 °C, and explosive limits in air between 0.7 and 5 (v/v).

A key engineering parameter to facilitate application of S-8, and mixtures of S-8 with JP-8 is the ADC. By adding the chemical family classifications to the data grid, the distillation curve becomes more information-rich. In Fig. 4, we present the classification results, as a function of distillate cut, for typical batches of JP-8 and S-8. The differences are striking. We note that S-8 has a high level of paraffinic species and very few aromatics (as expected from its natural gas feedstock), and JP-8 has a high aromatic content decreasing as distillation proceeds (as expected from its petroleum feedstock). We have found that this behavior is typical of kerosenes and diesel fuels [32–36], and is in contrast to that of gasolines, where one observes the aromatics to increase and aliphatics to decrease as the distillation proceeds [37]. The importance of this characterization technique stems from the required overall specifications for aviation fuels. Aromatics must be present to some extent in aviation fuels in order to meet the density specification. If present in excess, however, aromatics will produce soot and an overly luminous flame. The ability of the ADC to combine a check on the aromatic content and the physical property information provided by the boiling range is thus efficient and cost-effective.

2.3. Volatility and energy content

The ability to apply a detailed quantitative analysis to each distillate fraction offers the potential of assessing thermal properties such as energy content of a fuel. If the enthalpy of combustion

is known (or predictable) for the components of a mixture, the composite enthalpy of combustion of a mixture of these components can be derived (neglecting the enthalpy of mixing). We have demonstrated how this can be applied to the distillate fractions corresponding to the data grid of the distillation curve [38]. It is not necessary to identify all the components of the fraction; a substantial subset of the major constituents is adequate, and the uncertainty caused by the use of a subset is negligible (that is, less than the uncertainty resulting from the pure component enthalpy).

Continuing with the comparison of aviation fuel properties, one can appreciate that a major interest is the energy content. Moreover, since droplet combustion occurs inside the combustors of modern turbofan engines, the energy content as a function of distillate cut is very important. The shrinkage of a droplet in the combustor is accompanied by compositional changes, mirrored by the distillation curve. We illustrate the application of the ADC measurement of energy content with a comparison of different samples of Jet-A [29]. The ADC was applied to three different batches of Jet-A (designated numerically as 3638, 3602 and 4658) that are thought to represent the composition gamut very well. The sample labeled 4658 is the composite mentioned earlier. It is therefore considered to be the most representative of the three samples. The sample labeled 3638 was known to be unusual in that the aromatic content was lower than typical batches, while that labeled 3602 was unremarkable and typical. We noted a divergence in the distillation curves of these three fluids at the 70% fraction, so a quantitative analysis was done at this fraction for each fluid. We then applied our method to determine the enthalpy of combustion of this fraction, the results of which are shown as a histogram in Fig. 5, along with a comparison to the synthetic fluid made from natural gas, S-8. We were surprised to note a significant spread in the enthalpy values among these fluids. The mixed sample shows the highest energy content, while the atypical fluid 3638 shows the lowest. The combination of the distillation data grid with the composition analysis

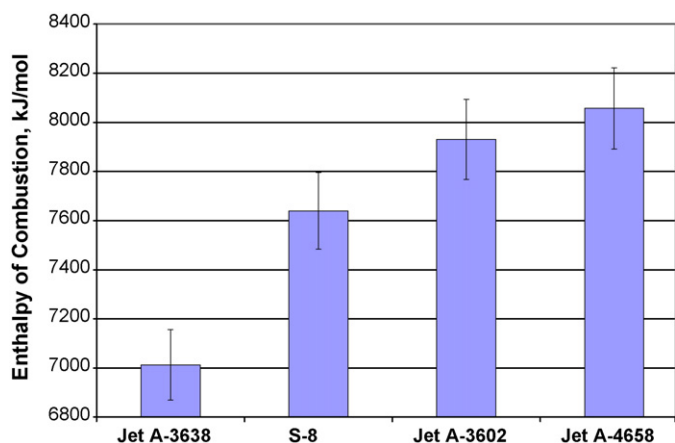


Fig. 5. The composite enthalpy of combustion of the 70% distillate fraction for three samples of Jet-A and the sample of S-8. The fluids are presented in increasing enthalpy of combustion.

and the enthalpic analysis permits a more complete understanding of the fuel properties, and how they relate to composition.

2.4. Tracking selected components

Finished fuels often incorporate additives for specific purposes, including oxygenating agents, antiknock agents, extenders, preservatives, antifoam and lubricity agents, and detergents. Some additives were mentioned above in our discussion of aviation kerosenes. While some of these are present at trace levels, others (especially oxygenates and extenders) are added in concentrations of 10% or higher. The development of models for the thermophysical properties of such fluids requires explicit knowledge of how the additives change the fundamental properties such as the volatility. We can use the ADC to unify these two important parameters.

Oxygenates added to gasoline to reduce carbon monoxide emissions are familiar, but various oxygenates have been added to diesel fuel to decrease (or eliminate) particulate formation. We have measured numerous gasoline and diesel fuel mixtures with oxygenates, including synthetics and biomass derived fluids [32,33,35]. Since many engine operation and environmental parameters depend on the distillation curve, the ability to relate the changing composition and actually model the fluid behavior is critical. In Fig. 6, we present the ADC results for mixtures of diesel fuel with three different concentrations of diethyl carbonate (DEC), a promising oxygenate [32]. DEC is used extensively as an ethylating agent in organic synthe-

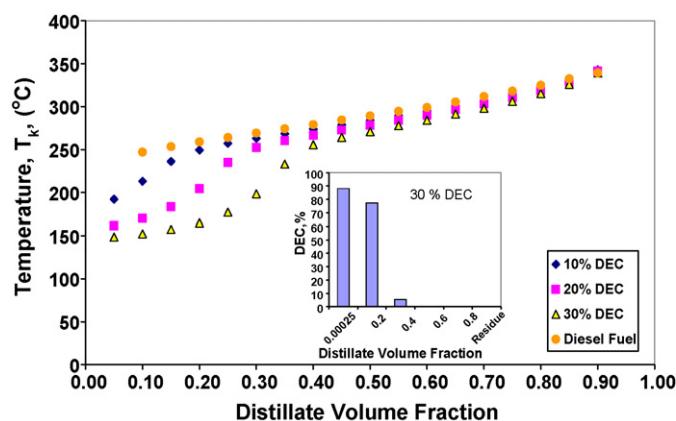


Fig. 6. The distillation curves of diesel fuel and diesel fuel with 10, 20, and 30% (v/v) of diethyl carbonate (DEC). The inset shows the concentration profile (in % (mass/mass)) of the additive as a function of distillate cut.

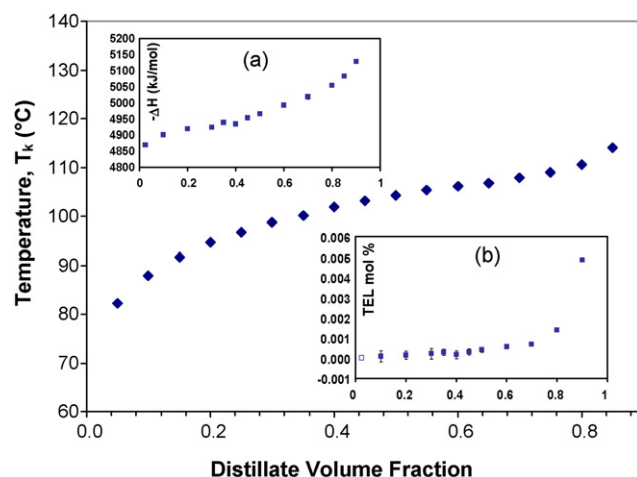


Fig. 7. Distillation curve of avgas 100LL with the enthalpy of combustion in inset (a), and the concentration of tetraethyl lead (TEL) in inset (b), both as a function of distillate cut.

sis (for example, it is used in the synthesis of the anticonvulsant drug Phenobarbital), and it is also used extensively as a solvent in the textile industry. It is biodegradable and insoluble in water. We note that in mixtures with diesel fuel, the DEC causes a significant inflection to lower temperatures. It is more volatile than most of the diesel fuel components, and even at a starting concentration of 30% (v/v), it has been removed from the diesel fuel by the 0.5 distillate fraction, at which point the distillation curves of the DEC mixture is approaching (but not merging with) that of diesel fuel. This is reflected in the inset, in which a quantitative analysis of the DEC in the distillate is provided, having been measured by GC-FID. Especially interesting is that the additive, although removed by a distillate fraction of 0.5, still apparently has an effect on the VLE late in the distillation. The vaporization of the lighter components of diesel fuel, which would ordinarily be found early in the distillation curve, is delayed by the presence of the additive. We will discuss this in more detail later in the section on thermodynamic modeling, however it is precisely this combination of temperature and composition information that permits a more complete understanding of the behavior of such complex mixtures.

Another instructive example of how we can track an additive through the distillation curve (but this time an additive concentration approaching the trace concentration level) comes from the measurement of the commercial aviation gasoline, avgas 100LL. Although motor fuels used today in the United States and Europe do not contain lead additives, much general aviation gasoline (avgas 100LL) still contains tetraethyl lead (TEL, CAS No. 78-00-2). Since TEL was banned from motor gasoline, avgas is now one of the largest contributors of lead in the atmosphere in many locations. Significant efforts have been made to develop a low cost, lead free alternative fuel to replace avgas 100LL for aircraft that use piston engines. The examination of avgas 100LL with the ADC provides the opportunity to ultimately develop an equation of state for avgas, and to track the presence of the lead compound through the full range of the distillation curve [39]. In Fig. 7, we apply the ADC to avgas 100LL [39]. The y-axis presents the thermodynamically consistent temperatures. In inset (a) we present the enthalpy of combustion as a function of distillate cut (from a quantitative analysis of each fraction). This allows the energy content to be related to the other fuel properties as a function of distillate cut. In inset (b), we present the composition profile of TEL as a function of distillate cut, which comes from specific trace analysis applied to the distillate cuts. We note that there is far more TEL in later distillate fractions.

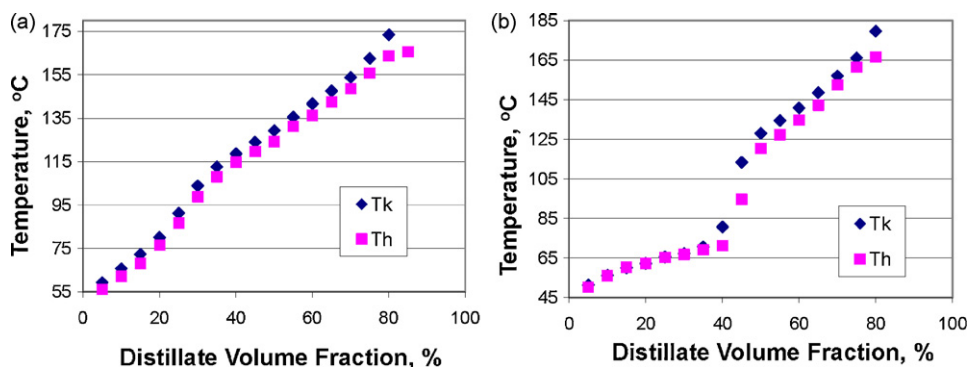


Fig. 8. Distillation curves of (a) 91 AI gasoline and (b) 91 AI gasoline with 15% (v/v) of methanol. The azeotropic convergence is caused by pairs of azeotropes forming between methanol and the some components of gasoline.

2.5. Detection of azeotropes

Azeotropic mixtures are among the most fascinating and at the same time the most complicated manifestations of phase equilibrium. They also play a critical role in many industrial processes (and the resulting products), especially separations.

As we noted earlier, the ADC measures two temperatures, T_k and T_h . Typically, during the measurement of a complex, multi-component fluid, the T_k measurement is higher than the T_h measurement by several (5–15) degrees Celsius. This must be the case, since the mass transfer driving force comes from the temperature differential between the kettle and the head. If one performs an ADC measurement on a pure fluid, the temperature difference between T_k and T_h is very small, no more than 0.1 °C (often less); the composition is not changing during the distillation. Moreover, the curve for a pure fluid is flat with zero slope. We would expect this difference in temperature differential and slope to be reflected in the distillation of an azeotrope, since where azeotropic pairs are present, the mixture behaves as a pure fluid. Mixtures of gasoline oxygenates in fact show this behavior, since the lower alcohols form azeotropes with many of the hydrocarbon components in gasoline [37]. In Fig. 8a, we show the distillation curves of a 91 AI (anti-knock index) premium, winter grade gasoline, presented in T_k and T_h . This fuel has no added oxygenate. We note for this complex, multi-component fluid that T_k is always higher than T_h by an average of 6.2 °C. In Fig. 8b we show the same gasoline with 15% (v/v) methanol. Two features are noteworthy. First we observe a flattening of the curve for distillate volume fractions up to approximately 40%, relative to that for the straight gasoline. This persists until the methanol has been distilled out of the mixture. Second, we also note

the convergence of T_k and T_h in this region, which we have called the azeotropic convergence. Here, the difference between T_k and T_h averages 0.3 °C, while subsequent to the azeotropic inflection, the difference increases to an average of 8.6 °C.

Sometimes the azeotropic convergence is not as dramatic as in the case of gasoline + methanol. This was illustrated in our measurements on mixtures of gasoline with the butanols [40]. This work stemmed from recognition of the many disadvantages of ethanol in fuel blends (including corrosivity toward ferrous metals, swelling of common elastomers used as seals in fuel systems, degradation of transfer lines, water absorption, phase separation, and a significantly lower energy content than typical gasoline) [32]. Mixtures with the butanols have been suggested as a possible alternative to avoid some of these difficulties. We applied the ADC to the four butanols, at mixture concentrations of 10, 20 and 30% (v/v). As an example, we show the curves for 1-butanol in Fig. 9, and with them we also show the T_k – T_h behavior for the 20% (v/v) mixture. We note that a convergence appears in the middle of the distillate range, corresponding with the vaporization of the 1-butanol. This results from the azeotropic binaries that occur between 1-butanol and the components of gasoline.

It might at first be surprising that the azeotropic convergence is very subtle, since our observation of the convergence with gasoline + methanol was very dramatic. In that case, in the azeotropic region, T_k and T_h converged to the extent that they overlaid on one another. The more subtle behavior here can be understood, however, by the respective phase diagrams of the butanols with the constituents of gasoline. The temperature of the azeotropic state point produced by the addition of methanol to a hydrocarbon is typically rather far from the boiling temperatures of the hydrocarbons

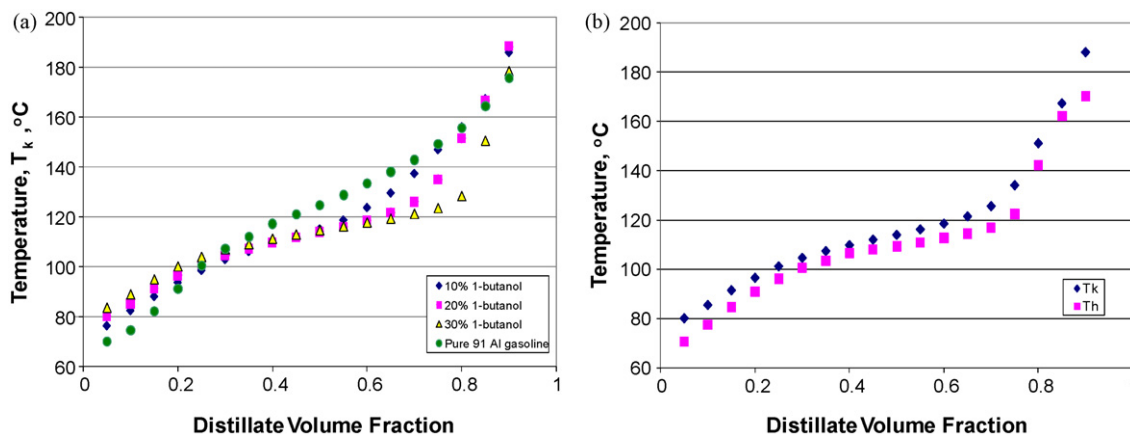


Fig. 9. (a) The distillation curves of gasoline in mixtures with 1-butanol at concentrations of 10, 20, and 30% (v/v). (b) The distillation curve of the gasoline + 1-butanol for a 20% mixture, plotted in T_k and T_h , showing the azeotropic convergence.

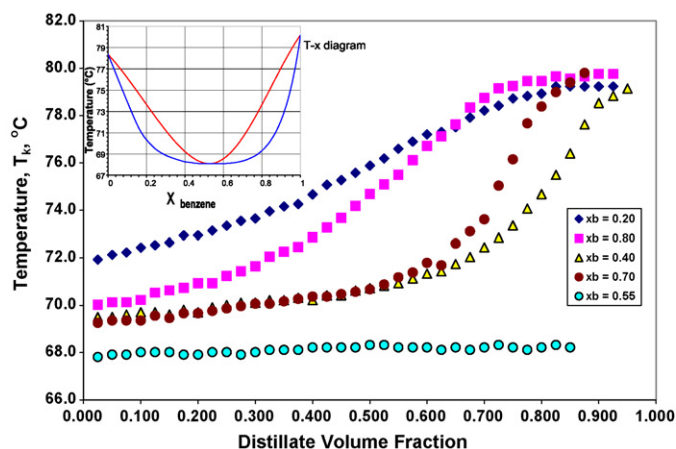


Fig. 10. A plot of the distillation curve data for binary mixtures of ethanol + benzene at benzene mole fractions $x_b = 0.20, 0.40, 0.55, 0.70$ and 0.80 . The inset shows the familiar T - x diagram for this mixture. The azeotrope exists at a benzene mole fraction of 0.55 .

themselves. For example, for cyclohexane, *n*-heptane, *n*-octane, and toluene, the temperature displacements are 53, 39, 63 and 47 °C, respectively. For 1-butanol with these same hydrocarbons, the displacements are 3, 7, 16 and 5 °C, respectively. Thus, the effect of 1-butanol on the mixture boiling points is clearly more subtle, illustrating the link between the ADC measurement and the vapor liquid equilibrium of the mixture.

2.6. Study of azeotropes

We can take the examination of azeotropes to a more fundamental level by examining some well known binary mixtures with the ADC. One of the most well studied mixtures is the minimum boiling binary azeotrope is that formed by benzene and ethanol. It is often presented in introductory texts as an instructional example because of the striking features and structure of the phase diagram (the temperature differences are significant, the two-phase region is large, and the azeotrope occurs nearly at the mid-point of the T - x diagram). This mixture is also industrially important in the formulation and design of oxygenated and reformulated gasolines. The T - x phase diagram of this binary, shown in the inset of Fig. 10, is anchored on the left side by the pure ethanol point (at a normal boiling temperature of 78.4 °C), and on the right side by the pure benzene point (at a normal boiling temperature of 80.1 °C). The bubble and dew point curves meet at the minimum located at 68.2 °C. Centered about the minimum on the bubble point curve is a relatively flat region where the slopes in either direction are gentle. These slopes become increasingly more pronounced as one proceeds away from the azeotrope. The dew point curves proceed from the azeotropic point to the pure component points in a more linear fashion with relatively constant slope.

Distillation curves are presented in this figure for binary mixtures with starting compositions of 0.20, 0.40, 0.55, 0.70 and 0.80 mol fraction of benzene (x_b) [41]. We note that the distillation curves for the starting compositions $x_b = 0.20$ and 0.40 converge at a temperature of 78.9 °C, while those at $x_b = 0.70$ and 0.80 converge at a temperature of 80.9 °C. These two different families of curves, which begin with starting compositions on either side of the azeotrope, converge to the appropriate pure component; 78.9 °C (for $x_b = 0.20$ and 0.40 , converging to ethanol) and 80.9 (for $x_b = 0.70$ and 0.80 converging to benzene). We note that the shapes of the curves for $x_b = 0.20$ and 0.80 are initially far steeper than those for $x_b = 0.40$ and 0.70 . This can be explained with reference to the T - x diagram. We note that the initial steepness of slope corresponds

with the pronounced increase in slope of the bubble point curve. Where the T - x diagram is steep, the distillation curve is correspondingly steep. This shape gives an indication of the deviations from Raoult's law, with steeper curves indicating larger deviations. For the mixture starting at a benzene mole fraction of 0.55, we note that the distillation curve is flat, behaving as a pure fluid at the azeotrope. We also note that the liquid and vapor compositions are the same. The ADC thus provides a simple and rapid avenue to the study of azeotropic mixtures. Each such curve can be completed in an hour with relatively simple instrumentation, whereas the T - x diagram would require many hours to measure in a specialized VLE apparatus.

2.7. Volatility and chemical stability

Biodiesel fuel has been the focus of a great deal of media attention and scientific research in the last several years as a potential replacement or extender for petroleum-derived diesel fuel. The major constituents (fatty acid methyl esters, FAMES) of pure biodiesel are generally relatively few, consisting mainly of methyl palmitate, methyl stearate, methyl oleate, methyl linoleate, and methyl linolenate. As a fuel for compression ignition engines, biodiesel fuel has several advantages (renewable, increased lubricity, non-carcinogenic, non-mutagenic, biodegradable, decreased carbon monoxide, unburned hydrocarbon, and particulate matter emission). There are also some serious disadvantages to biodiesel fuel (increased NO_x emissions, moisture absorption during storage, and chemical instability). The last item is especially problematic at higher temperatures, although the instability in storage has received more attention. We found in earlier work on biodiesel fuel (B100) that the thermal and oxidative instability of this fluid prevented the measurement of a distillation curve with our usual ADC approach; discrepancies in temperature of up to 20 °C were observed between successive measurements. The addition of an argon gas sparge incorporated into the distillation flask eliminated the problem, and allowed the measurement of highly reproducible distillation curves [42,43]. Since it is possible to quantitatively assess the "tightening" of replicate distillation curve measurement upon the addition of the sparge, we can use this change as a means of assessing the thermal and oxidative stability of the fluids being measured. We used three statistical descriptors of the improved curve-to-curve repeatability: the average range in temperature, the average standard deviation in temperature, and the area subtended. We found that these measures correlated quantitatively with improved thermal and oxidative stability and thus provide a measure of stability.

We then used the ADC as described above to test the efficacy of stabilizing additives on sensitive fluids such as B100 [44]. In particular, we tested three hydrogen donor additives: tetrahydroquinoline (THQ), *t*-decalin and tetralin (the classical donor solvent is composed of a saturated ring attached to an aromatic ring). Hydrogen donors are fluids or solvents that are capable of providing hydrogen to enable the conversion of heavier residuals into distillable fractions. They act to cap aliphatic radicals formed at temperatures in excess of 300 °C, and typically form C2 and C3 alkyl aromatic compounds. In Fig. 11, we present the distillation curve of B100 stabilized with 1% (v/v) THQ, and note that the repeatability of three successive curves is approximately 1.6 °C. This is a significant improvement from the unstabilized fluid (although not as significant as with the argon sparge). We track the concentration of THQ in the distillate in the inset, with the composition-explicit data channel of the ADC. We note that the stabilization effect is greatest earliest in the curve, when the concentration of THQ is highest. The THQ decomposes and also distills out of the mixture during the course of the distillation, and its effect naturally decreases. Of the three stabilizers examined, the THQ and *t*-decalin perform

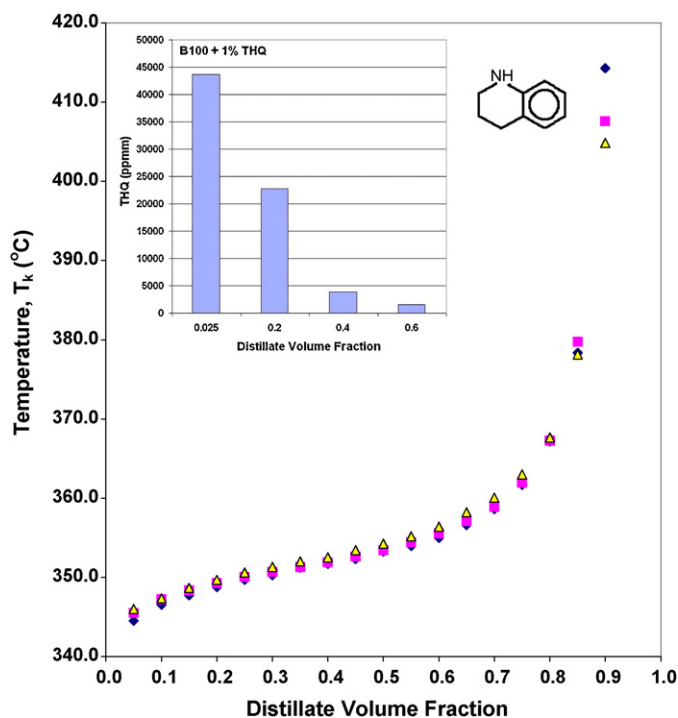


Fig. 11. Three successive distillation curves of B100 biodiesel fuel with 1% THQ (structure provided) stabilizing additive. The inset tracks the concentration (in ppm by mass) of THQ present in the distillate.

similarly; tetralin also resulted in stabilization, but with less effectiveness. Interestingly, this result parallels kinetics measurements performed on aviation fuels stabilized with these additives [45–47].

2.8. Volatility and corrosivity

Crude oil is an economic driving force in the developed world. Many properties of crude oil (color, viscosity, and amount and type of impurities) are dependent on its source. Impurities of primary concern are sulfur species, which are often corrosive. Crude oils containing relatively few sulfur impurities are referred to as “sweet”; they are considered “sour” if they contain large amounts of sulfur impurities. The corrosivity of crude oil streams is always an important issue, one that can account for serious financial liabilities by producers and refiners. The corrosivity of certain sulfur species in fluids is determined by ASTM test methods D-1838 or D-130, the copper strip corrosion test (CSCT) [48–54]. A strip of cleaned, polished copper is placed in a vessel and then filled with an appropriate quantity of the fluid to be tested. The filled vessel is then maintained at an elevated temperature for a predetermined amount of time, and the strip is removed from the fluid and immediately rated by comparison with a lithographed standard. There are four levels of increasing corrosion on the standard, with level one corresponding to slight tarnishing and level four corresponding to severe corrosion.

Although the CSCT is a well-established standard, it is both qualitative and subjective. We improved the interpretation of CSCT by analyzing strips in a mathematical color space, specifically $L^*a^*b^*$ color space (the most complete, perceptually linear color model) [55]. We adapted the dimensionless L^* axis of this space, which describes the “lightness” of an image, to measure the corrosion of copper strips. Lightly tarnished strips generally have high L^* values (180–210), while severely tarnished strips generally have low L^* values (120–150). While the usual CSCT was designed for 30 mL fluid samples and large copper strips (75 mm × 12.5 mm, up to 3.0 mm thick), we used very small, circular copper coupons that

fit in the bottom of GC autosampler vials. Moreover, the symmetric circular geometry facilitates the analysis of the images with $L^*a^*b^*$ color space, and the small size of the coupons can actually facilitate corrosion testing [56].

We applied the ADC approach to several crude oils, and sand crude [57,58]. In a more exotic application, we measured a “crude oil” made from swine manure [16]. To make the oil, swine manure, suspended in water, is pressurized in a reactor with CO and heated to approximately 300 °C. The overall yield of oil from the reactor is approximately 11% (mass/mass). In Fig. 12, we present a distillation curve, along with the CSCT results. Insets show FTIR spectra of an early and late fraction, and GC-MS of a mid-fraction. The relatively high water content of this oil causes the distillation temperatures to start at a low value and jump when the organics begin to distill. The high water content early in the distillation is reflected in the FTIR data, as is the high hydrocarbon content that develops later. The CSCT shows the fluid to be somewhat corrosive through the distillation curve. The L^* values (not listed here) correlated with the CSCT ratings.

Analyses by GC-MS showed that the swine manure crude is a very complex mixture: even when investigating only the main peaks (with an abundance above 1%), 83 different organic compounds were identified. The main peaks from the low boiling region distillate samples were identified as nitrogenous heterocycles: substituted pyrazines and pyrroles. Also identified in the first drop were thiophenes. The sulfur in the thiophenes was also quantitated by GC-SCD. The high boiling fractions were dominated by long-chain hydrocarbons; fluids from octane to octadecane were identified. In addition to these hydrocarbons, an interesting component identified on the basis of its mass spectrum was coprostanol. Coprostanol is the parent hydrocarbon of coprostanol (also called coprosterol, CAS No. 360–68–9), which is a main sterol found in swine fecal matter. Its presence indicates that the thermal conversion conditions of swine manure to crude oil were not sufficient to thermally crack this polycyclic compound.

Unlike our experiences with finished fuels or other crudes, a large fraction of particulate char remained after distillation. The ADC allows recovery and analysis of this material. A powder X-ray diffraction pattern was inconclusive. Consequently, the char was analyzed with instrumental neutron activation analysis and cold neutron prompt gamma activation analysis. These complementary neutron activation analysis techniques detected the presence of: Fe, Zn, Ag, Co, Cr, La, Sc, W, and very small amounts of Au and Hf. Metals such as Fe have been found elsewhere in swine manure and lagoon sludge.

3. Thermodynamic modeling

Thus far in the discussion, we have focused on the analytical applications of the ADC. An important contribution to the concept of petroleomics (as advanced by Marshall and Rogers), however, is the ability to use the information to advance the applied theory of complex fluids so as to describe and predict the physical properties of the mixture and its components [59]. In their landmark review, Marshall and Rogers defined the term as the relationship between the chemical composition of a fossil fuel and its properties and reactivity. Establishing this relationship has been more difficult than the detailed analysis of the components in fossil fuels. Since the ADC produces thermodynamically consistent temperatures along with the relevant composition picture, it is ideally suited for the development of such complex fluid theory. The basic idea in our approach is to represent the molar Helmholtz energy, a , of a mixture as a sum of an ideal contribution, a^{idsol} , and an excess contribution a^{excess} :

$$a = a^{\text{idsol}} + a^{\text{excess}}, \quad (1)$$

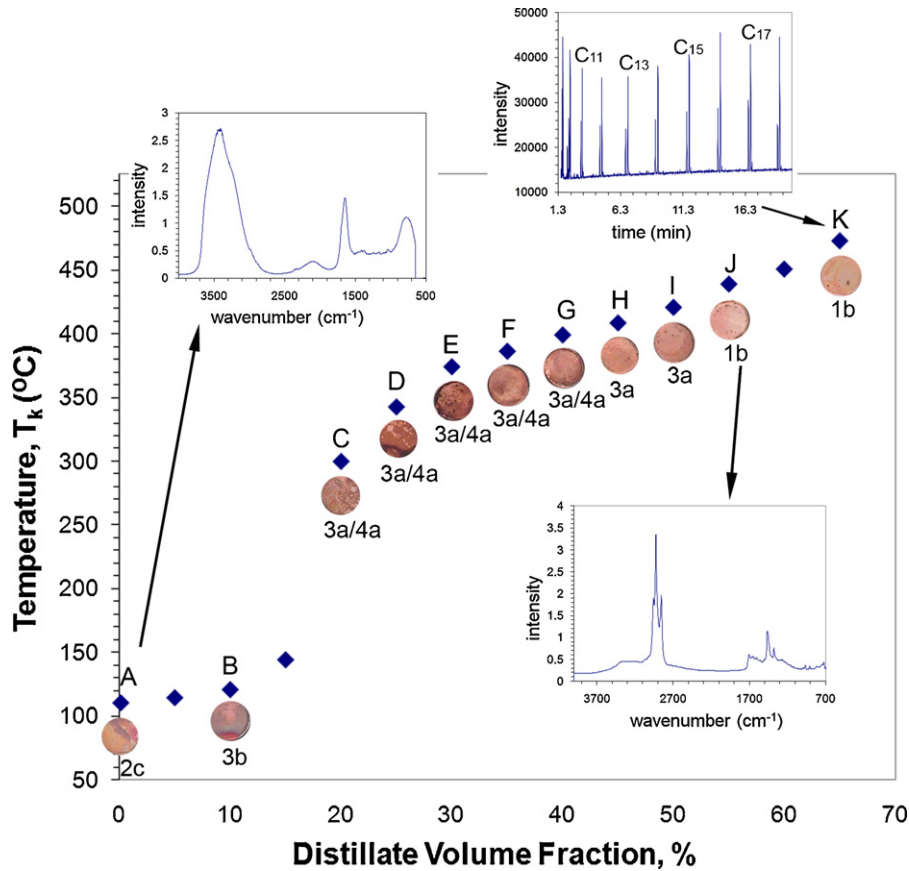


Fig. 12. The distillation curve of the crude oil made from swine manure is shown by the diamonds, along with the CSCT coupons for each fraction. The FTIR spectra for an early and a late fraction, and GC-MS results for a middle fraction, are shown in the insets.

$$a^{\text{idsol}} = \sum_{j=1}^m x_j [a_j^0(\rho, T) + a_j^r(\delta, \tau) + RT \ln x_j], \quad (2)$$

$$a^{\text{excess}} = RT \sum_{i=1}^{m-1} \sum_{j=i+1}^m x_i x_j F_{ij} \sum_k N_k \delta^{d_k} \tau^{t_k} \exp(-\delta^{l_k}), \quad (3)$$

where ρ and T are the mixture molar density and temperature, δ and τ are the reduced mixture density and temperature, m is the number of components, a_i^0 is the ideal gas Helmholtz energy of component i , a_i^r is the residual Helmholtz energy of component i , the x_i are the mole fractions of the constituents of the mixture, d_k , t_k , l_k and N_k are coefficients found from fitting experimental data, F_{ij} is an interaction parameter, and R is the universal gas constant [60]. Mixing rules are used to determine the reducing parameters ρ_{red} and T_{red} for the mixture that are defined as

$$\delta = \frac{\rho}{\rho_{\text{red}}}, \quad (4)$$

$$\tau = \frac{T_{\text{red}}}{T}, \quad (5)$$

$$\rho_{\text{red}} = \left[\sum_{i=1}^m \frac{x_i}{\rho_{c_i}} + \sum_{i=1}^{m-1} \sum_{j=i+1}^m x_i x_j \xi_{ij} \right]^{-1}, \quad (6)$$

$$T_{\text{red}} = \sum_{i=1}^m x_i T_{c_i} + \sum_{i=1}^{m-1} \sum_{j=i+1}^m x_i x_j \varsigma_{ij}, \quad (7)$$

where ξ_{ij} and ς_{ij} are binary interaction parameters that define the shapes of the reducing temperature and density curves, and T_{red} and ρ_{red} are the reduced temperature and density.

The model has three binary interaction parameters for each component pair, ξ_{ij} , ς_{ij} and F_{ij} that can be determined by fitting experimental data. If the constituent fluids are chemically similar, the excess contribution can be set to zero (i.e., $F_{ij}=0$), and the ξ_{ij} interaction parameter to zero, resulting in a simpler model with only one binary interaction parameter, ς_{ij} . Previous studies on refrigerant mixtures have shown that ς_{ij} is the most important binary parameter. This parameter can be found by fitting binary mixture data, or when data are unavailable, the following predictive scheme is used:

$$\varsigma_{ij} = \frac{T_{c_2}}{T_{c_1}} (40.4 - 25.03 \times 2^s) \quad (8)$$

where

$$s = \left(\frac{T_{c_1}}{T_{c_2}} \frac{\rho_{c_2}}{\rho_{c_1}} \frac{\omega_2}{\omega_1} \right), \quad (9)$$

where the fluid with the smaller dipole moment is designated as fluid “1”, and ω is the acentric factor [61].

The model for calculating the transport properties of a mixture is an extended corresponding states method [62]. In this approach, the viscosity or thermal conductivity of a mixture is calculated in a two-step procedure. First, mixing and combining rules are used to represent the mixture in terms of a hypothetical pure fluid, then the properties of the hypothetical pure fluid are determined by mapping onto a reference fluid through the use of “shape factors”; details are given elsewhere. For both refrigerant mixtures and mixtures of natural gas components the viscosity and thermal conductivity are typically represented to within 5–10%. The two models discussed briefly above, the Helmholtz energy mixing model for thermodynamic properties and the extended corresponding states model for viscosity and thermal conductivity, are

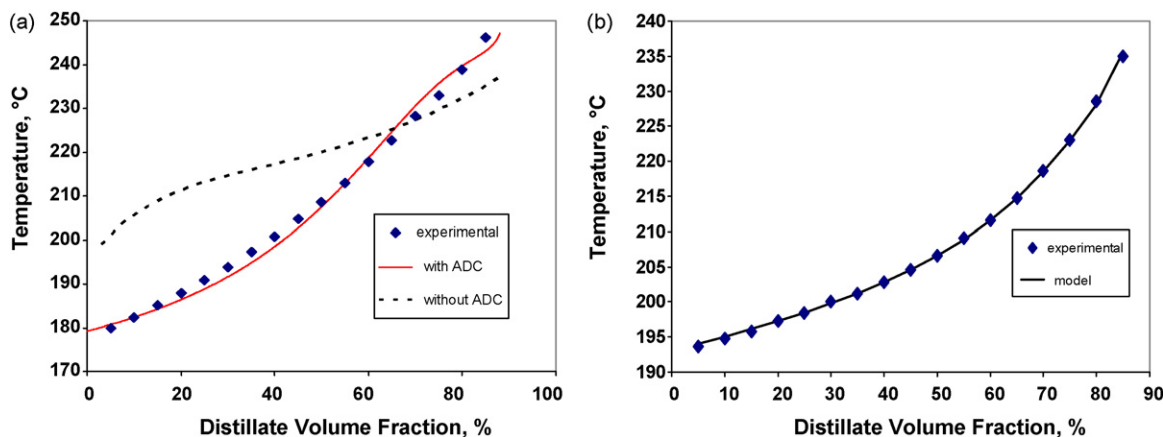


Fig. 13. A plot showing the distillation curves modeled with the Helmholtz equation of state as compared with experimental data. The plot shown in (a) is for the synthetic aviation turbine fuel S-8, made from natural gas, and shows the model with and without the incorporation of the ADC data. The plot shown in (b) is for a coal-derived liquid turbine fuel in which the Helmholtz equation of state is used predictively to generate the distillation curve.

implemented in NIST's REFPROP computer program. This program contains highly accurate equations of state for pure fluids, including some adopted as international standards [60].

We can use the theoretical formalism presented above in different ways. First, we can correlate experimental property data, producing a model to represent the data within experimental uncertainty. Second, we can use the model predictively to estimate property values, based on limited experimental data. With the ADC as a primary experimental input, we have used both of these approaches.

Returning to the synthetic aviation fuel S-8 discussed earlier, we can represent the composition of the fluid with a surrogate mixture with components representing families of compounds found in S-8. Then, correlating measured density, heat capacity, sound speed, viscosity and thermal conductivity, it is possible to model the properties of the mixture. Without the advanced distillation curve as an input, however, the ability of the model to represent volatility is severely flawed [17]. We show in Fig. 13a the experimental measurements, and calculated distillation curves developed with the Helmholtz model with and without the ADC data as an input. Including the distillation curve in the model development allows correlation of the volatility to within experimental uncertainty, while failing to do so results in a physically unrealistic representation.

We can also use the formalism presented above in a predictive fashion, whereby we use a chemical analysis along with the advanced distillation curve to predict the remaining physical property information (density, sound speed and viscosity). As an example, we study another synthetic substitute for JP-8, a blended coal-derived fluid (CDF) made from a significant fraction of coal liquids and light cycle oil, a by-product of catalytic cracking units in petroleum refining [18,31]. The resulting mixture was treated to increase the number of carbon–hydrogen bonds by hydroprocessing at high temperature and pressure. The fluid is intended for high chemical stability up to 480 °C (900 °F, hence the alternative name of the prototype, JP-900). The chemical analysis allowed the development of a five-component surrogate, and the resulting mixture model calculated the distillation curve very well as shown in Fig. 13b. Moreover, the mixture model can represent other physical properties to within experimental uncertainty, realizing that such data are very limited.

In the discussion earlier on the oxygenating additives for diesel fuel, we noted that in some cases, the additive has an effect on the volatility even after the additive has been completely removed (by distillation) from the mixture. This was illustrated with diethyl

carbonate, but we have observed the same effect with many more volatile additives that vaporize early in the distillation. This occurs because the energy being applied to the solution during the distillation is being used to vaporize the additive, and the lighter components of the fluid undergo delayed vaporization. We can use the thermodynamic models to demonstrate this, and predict the vaporization of the relevant species during the course of distillation. To do this we construct a very simplified surrogate mixture for diesel fuel and dimethyl carbonate (DMC), as listed in Table 1 [32]. We choose DMC for this illustration, since the effect is dramatic and easily demonstrated on a plot. We can calculate the distillation curves for the three mixtures, and indeed the curves will not completely merge, even after the DMC has vaporized. Fig. 14a and b shows further calculations from our surrogate model, specifically tracking how the composition of the liquid and vapor phases change as the distillation proceeds. The compositions of DMC, *n*-nonane (the lightest component in the surrogate diesel) and *n*-hexadecane (the heaviest component in the surrogate diesel) are shown. Fig. 14a shows that the concentration of *n*-nonane is affected significantly by the additive, while the *n*-hexadecane is affected to a much lesser extent. This behavior is shown for two initial concentrations of dimethyl carbonate (30% (v/v), and 10% (v/v)) as described in Table 1. In Fig. 14a, the peak in the vapor phase concentration of nonane is delayed, so that the removal of *n*-nonane from the liquid phase is also delayed. The difference in the 10 and 30% mixtures is dramatic, with the vaporization of *n*-nonane being delayed much later into the distillation than the 10% mixture. This results in the distillation curves approaching, but never merging, even though the dimethyl carbonate itself has vaporized.

Table 1

Constituents and mole fractions used in the simple surrogate models developed to simulate the behavior of the distillation curves of diesel fuel with dimethyl carbonate (DMC).

Compound	Mole fraction composition of the 10% (v/v) DMC mixture	Mole fraction composition of the 20% (v/v) DMC mixture	Mole fraction composition of the 30% (v/v) DMC mixture
<i>n</i> -Nonane	0.0200	0.0160	0.0140
<i>n</i> -Decane	0.0400	0.0310	0.0280
<i>n</i> -Undecane	0.1000	0.0790	0.0700
<i>n</i> -Dodecane	0.4046	0.3178	0.2848
<i>n</i> -Tridecane	0.1000	0.0790	0.0700
<i>n</i> -Tetradecane	0.0400	0.0310	0.0280
<i>n</i> -Pentadecane	0.0400	0.0310	0.0280
<i>n</i> -Hexadecane	0.0200	0.0160	0.0140
Dimethyl carbonate	0.2354	0.3992	0.5368

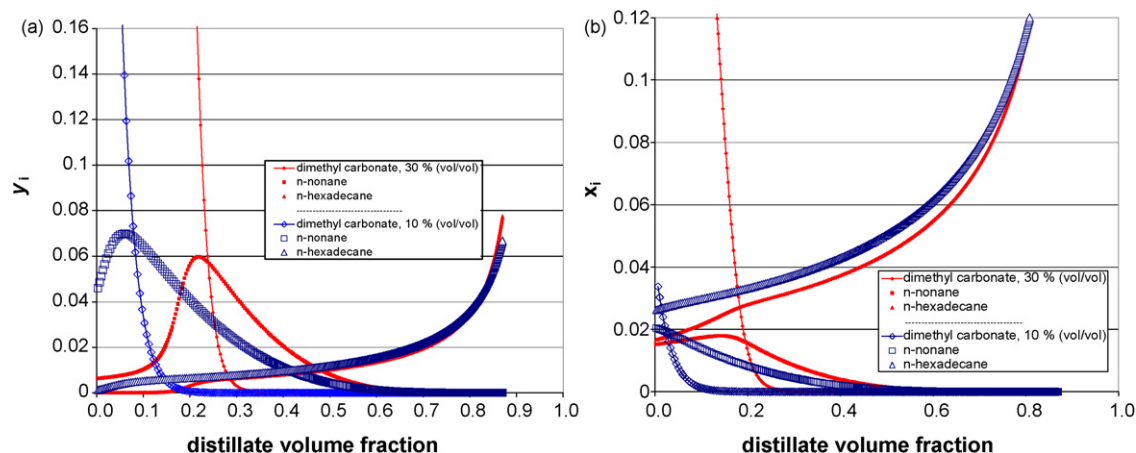


Fig. 14. (a) Calculated distillation curves (expressed as mole fractions of vapor, y_i) for the mixture of 30% (v/v) dimethyl carbonate and 10% (v/v) dimethyl carbonate in the surrogate summarized in Table 1. (b) Calculated distillation curves (expressed as mole fractions of liquid, x_i) for the surrogate.

4. Conclusion

In this review, we have discussed the salient features of the composition-explicit or advanced distillation curve approach for the measurement of complex, multi-component fluids. The method bridges the gap between a chemical analysis protocol and a thermophysical property measurement in a relational manner. Thus, analytical information can be used to enhance a measure of fluid volatility, and vice versa. The result is a powerful method that can be used to characterize fluids and in the development of thermophysical property models.

References

- [1] Separation and Purification; Critical Needs and Opportunities, Committee on Separation Science and Technology, Board of Chemical Sciences and Technology, Commission on Physical Science, Mathematics and Resources, National Research Council, 1987.
- [2] J.R. Conder, C.L. Young, *Physicochemical Measurements by Gas Chromatography*, John Wiley and Sons, Chichester, 1979.
- [3] H.Z. Kister, *Distillation Operation*, McGraw-Hill, New York, 1988.
- [4] H.Z. Kister, *Distillation Design*, McGraw-Hill, New York, 1991.
- [5] C.P. Angelos, S.V. Bhagwat, M.A. Matthews, *Fluid Phase Equilib.* 72 (1992) 182.
- [6] M.S. Peters, K.D. Timmerhaus, R.E. West, *Plant Design and Economics for Chemical Engineers*, McGraw-Hill, New York, 2002.
- [7] M.R. Riazi, *Characterization and Properties of Petroleum Fractions*, ASTM MNL50, American Society for Testing and Materials, West Conshohocken, PA, 2005.
- [8] M.R. Riazi, H.A. Al-Adwani, A. Bishara, *J. Petrol. Sci. Eng.* 42 (2004) 195.
- [9] D.A. Stark, *Notes on Petroleum Processing*, University of Notre Dame, 1998, <http://www.nd.edu/~msen/Teaching/DirStudies/Petroleum>.
- [10] ASTM Standard D 86-04b, *Standard Test Method for Distillation of Petroleum Products at Atmospheric Pressure*, ASTM International, West Conshohocken, PA, 2004.
- [11] T.J. Bruno, *Ind. Eng. Chem. Res.* 45 (2006) 4371.
- [12] T.J. Bruno, B.L. Smith, *Ind. Eng. Chem. Res.* 45 (2006) 4381.
- [13] T.J. Bruno, *Sep. Sci. Technol.* 41 (2006) 309.
- [14] B.L. Smith, T.J. Bruno, *Int. J. Thermophys.* 27 (2006) 1419.
- [15] T.J. Bruno, A. Wolk, A. Naydich, *Energy Fuels* 23 (2009) 3277.
- [16] L.S. Ott, B.L. Smith, T.J. Bruno, *Fuel* 87 (2008) 3379.
- [17] M.L. Huber, B.L. Smith, L.S. Ott, T.J. Bruno, *Energy Fuels* 22 (2008) 1104.
- [18] M.L. Huber, E.W. Lemmon, V. Diky, B.L. Smith, T.J. Bruno, *Energy Fuels* 22 (2008) 3249.
- [19] M.L. Huber, E. Lemmon, L.S. Ott, T.J. Bruno, *Energy Fuels* 23 (2009) 3083.
- [20] T.J. Bruno, *Anal. Chem.* 58 (1986) 1595.
- [21] T.J. Bruno, *J. Chem. Educ.* 64 (1987) 987.
- [22] T.J. Bruno, American Laboratory, Shelton, CT, United States, 1993, p. 16.
- [23] A. Crafts, *Berl. Berichte.* 20 (1897) 709.
- [24] L.S. Ott, B.L. Smith, T.J. Bruno, *J. Chem. Thermodynam.* 40 (2008) 1352.
- [25] S. Young, *Proc. Chem. Soc.* 81 (1902) 777.
- [26] S. Young, *Fractional Distillation*, Macmillan and Co., Ltd., London, 1903.
- [27] S. Young, *Distillation Principles and Processes*, Macmillan and Co., Ltd., London, 1922.
- [28] Purchase Description, RP-1, Federal Business Opportunities, <http://fs2.epa.gov/EPSData/DLA/Synopses/12671/SP0600-03-R-0322/rp-1sol.pdf>, 2003.
- [29] B.L. Smith, T.J. Bruno, *Ind. Eng. Chem. Res.* 46 (2007) 310.
- [30] B.L. Smith, T.J. Bruno, *J. Propul. Power* 24 (2008) 619.
- [31] B.L. Smith, T.J. Bruno, *Energy Fuels* 21 (2007) 2853.
- [32] T.J. Bruno, A. Wolk, A. Naydich, M.L. Huber, *Energy Fuels* 23 (2009) 3989.
- [33] L.S. Ott, B.L. Smith, T.J. Bruno, *Energy Fuels* 22 (2008) 2518.
- [34] L.S. Ott, A. Hadler, T.J. Bruno, *Ind. Eng. Chem. Res.* 47 (2008) 9225.
- [35] B.L. Smith, L.S. Ott, T.J. Bruno, *Environ. Sci. Technol.* 42 (2008) 7682.
- [36] T.M. Lovestead, T.J. Bruno, *Energy Fuels* 23 (2009) 3637.
- [37] B.L. Smith, T.J. Bruno, *Ind. Eng. Chem. Res.* 46 (2007) 297.
- [38] T.J. Bruno, B.L. Smith, *Energy Fuels* 20 (2006) 2109.
- [39] T.M. Lovestead, T.J. Bruno, *Energy Fuels* 23 (2009) 2176.
- [40] T.J. Bruno, A. Wolk, A. Naydich, *Energy Fuels* 23 (2009) 2295.
- [41] A.B. Hadler, L.S. Ott, T.J. Bruno, *Fluid Phase Equilib.* 281 (2009) 49.
- [42] L.S. Ott, T.J. Bruno, *Energy Fuels* 22 (2008) 2861.
- [43] B.L. Smith, L.S. Ott, T.J. Bruno, *Ind. Eng. Chem. Res.* 47 (2008) 5832.
- [44] T.J. Bruno, A. Wolk, A. Naydich, *Energy Fuels* 23 (2009) 1015.
- [45] T.J. Bruno, *Process Control and Quality*, 1992, p. 195.
- [46] J.A. Widegren, T.J. Bruno, *Energy Fuels*, submitted for publication.
- [47] J.A. Widegren, T.J. Bruno, *Proceedings of 4th Liquid Propulsion Subcommittee, JANNAF*, December, 2008.
- [48] ASTM D 130, *Standard Test Method for Corrosiveness to Copper from Petroleum Products by Copper Strip Test*, ASTM International, West Conshohocken, PA, 2004.
- [49] ASTM D 1838-07, *Standard Test Method for Copper Strip Corrosion by Liquefied Petroleum (LP) Gases*, ASTM International, West Conshohocken, PA, 2007.
- [50] W.C. Andersen, A.I. Abdulagatov, T.J. Bruno, *Energy Fuels* 17 (2003) 120.
- [51] W.C. Andersen, T.J. Bruno, *Abstracts of Papers 225th ACS National Meeting*, New Orleans, LA, United States, 23–27 March, ETR, 2003.
- [52] W.C. Andersen, T.J. Bruno, *Ind. Eng. Chem. Res.* 42 (2003) 971.
- [53] W.C. Andersen, T.J. Bruno, *Ind. Eng. Chem. Res.* 42 (2003) 963.
- [54] P.D.N. Svoronos, T.J. Bruno, *Ind. Eng. Chem. Res.* 41 (2002) 5321.
- [55] W.C. Andersen, G.C. Straty, T.J. Bruno, *Proceedings of the GTI natural Gas Technologies Conference and Exhibition*, Phoenix, AZ, 2004.
- [56] L.S. Ott, T.J. Bruno, *J. Sulfur Chem.* 28 (2007) 493.
- [57] L.S. Ott, T.J. Bruno, *Energy Fuels* 21 (2007) 2778.
- [58] L.S. Ott, B.L. Smith, T.J. Bruno, *Fuel* 87 (2008) 3055.
- [59] A.G. Marshall, R.P. Rodgers, *Acc. Chem. Res.* 37 (2004) 53.
- [60] E.W. Lemmon, R.T. Jacobsen, *J. Phys. Chem. Ref. Data* 33 (2004) 593.
- [61] E.W.M. Lemmon, M.O. McLinden, *Proceedings of the Thermophysical Properties and Transfer Processes of New Refrigerants Conference*, International Institute of Refrigeration, Paderborn, Germany, 2001, p. 23.
- [62] M.L. Huber, A. Lasecke, R.A. Perkins, *Ind. Eng. Chem. Res.* 42 (2003) 3163.